

Distributed Power Allocation for Cooperative Wireless Network Localization

Wenhan Dai, *Student Member, IEEE*, Yuan Shen, *Member, IEEE*, and Moe Z. Win, *Fellow, IEEE*

Abstract—Device-to-device (D2D) communication in cellular networks is a promising concept that permits cooperation among mobile devices not only to increase data throughput but also to enhance localization services. In those networks, the allocation of transmitting power plays a critical role in determining network lifetime and localization accuracy. Meanwhile, it is a challenging task for implementation in cooperative networks, since each device has only imperfect estimates of local network parameters in distributed settings. In this paper, we establish an optimization framework for robust power allocation in cooperative wireless network localization. We then develop distributed power allocation strategies via relaxation of the original problem. In particular, we decompose the power allocation problem into infrastructure and cooperation phases, show the sparsity property of the optimal power allocation, and develop efficient power allocation strategies. Simulation results show that these strategies can achieve significant performance improvement compared to the uniform strategies in terms of localization accuracy.

Index Terms—Convex optimization, cooperative techniques, localization, power allocation, robust optimization.

I. INTRODUCTION

LOCATION-AWARENESS of mobile devices is essential for many emerging applications and services in wireless networks, such as indoor navigation, asset tracking, social networking, and environmental monitoring [1]–[9]. Conventional techniques are not adequate for providing seamless and high-accuracy location awareness in harsh environments. For example, the global positioning system (GPS) does not operate well indoors or in urban canyons due to signal blockage [10]; and the techniques that rely on cellular network infrastructures cannot provide satisfactory localization accuracy [7]. This inadequacy has motivated recent research activities in localization for wireless networks [11]–[24].

Typical localization systems for wireless networks employ two types of nodes, i.e., anchors (infrastructure with known positions) and agents (mobile devices with unknown positions). Conventionally, agents aim to infer their positions based on

Manuscript received May 20, 2013; revised November 15, 2013; accepted August 5, 2014. This research was supported, in part, by the Air Force Office of Scientific Research under Grant FA9550-12-0287, the Office of Naval Research under Grant N00014-11-1-0397, and the MIT Institute for Soldier Nanotechnologies. The material in this paper was presented, in part, at the IEEE International Conference on Communications, Sydney, Australia, June 2014.

W. Dai and M. Z. Win are with the Laboratory for Information and Decision Systems (LIDS), Massachusetts Institute of Technology, Cambridge, MA 02139, USA (e-mail: {whdai, moewin}@mit.edu).

Y. Shen is with the Laboratory for Information and Decision Systems (LIDS), Massachusetts Institute of Technology, Cambridge, MA 02139, USA, and also with the Electronic Engineering Department, Tsinghua University, Beijing 100084, China (e-mail: shenyuan@mit.edu).

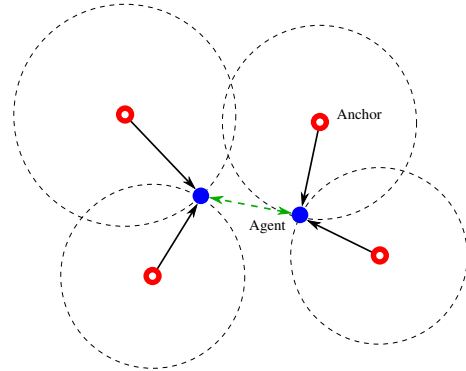


Fig. 1. Cooperative wireless network localization: the anchors are infrastructures such as cellular base stations and GPS satellites, and the agents are mobile devices. The agents infer their positions by making range measurements with neighboring anchors and agents.

range measurements to the anchors [6]–[8].¹ With the emergence of device-to-device (D2D) communication, each agent can make additional range measurements with its neighboring agents, and cooperates with them for positional inference. Such cooperation can significantly improve localization performance by virtue of sharing position information among neighbors [25]–[28], thus circumventing the use of high-power, high-density anchor deployment required for high-accuracy non-cooperative localization. For example, in Fig. 1, the agent’s cooperation enables both agents to determine their positions, while neither agent can trilaterate its position unless it can make range measurements with more anchors.

Localization accuracy in wireless networks is determined by the network topology and the accuracy of range measurements, where the latter depends on transmitting power, signal bandwidth, and channel condition [8]. Allocation of the transmitting power plays a critical role in wireless network localization (WNL) since it affects network lifetime in addition to localization accuracy. In fact, power allocation strategies have been shown to significantly improve the localization accuracy and reduce the power consumption in non-cooperative localization networks [29]–[31].

Existing studies on power allocation for WNL considered only the non-cooperative cases in the absence of D2D communication [32]–[35]. The power allocation problems in these studies were formulated as various optimization programs that minimize the localization errors subject to a given transmitting power constraint, or vice versa. In particular, the power

¹The range measurement (made by an agent) to a node refers to the measurement of the distance between the agent and the node.

allocation problems were investigated for wireless sensor networks in [32] and for multiple-antenna radar networks in [33]. Both studies employed the Cramér–Rao Bound as the performance metric and relaxed the original problems into convex programs. The authors in [34] adopted the squared position error bound (SPEB) as the performance metric and demonstrated that the power allocation problem for WNL can be transformed into semi-definite programs (SDPs). Using two important functional properties of the SPEB, recent work [35] showed that the power allocation problems can be transformed into second-order cone programs (SOCPs), which have more efficient solvers than SDPs.

Little is known about optimizing the allocation of the transmitting power among anchors and agents in cooperative WNL. Due to the additional range measurements between agents in cooperative settings, the expression for the agents' SPEBs has a much more complicated structure than its non-cooperative counterpart [25], hindering the design and analysis of power allocation strategies. Moreover, distributed power allocation strategies are more desirable than centralized ones, since the latter requires the parameters of the entire network. Designing such distributed power allocation strategies brings another layer of difficulty because the location information of the agents is interrelated over the entire network while only local network parameters are available at each agent [36]–[39]. In addition, it is essential to design robust strategies that can cope with the uncertainty of network parameters since, in practice, perfect estimates of such parameters are often unavailable. Therefore, the goal of this work is to design distributed power allocation strategies for cooperative WNL under network parameter uncertainty.

In this paper, we establish an optimization framework for robust power allocation in cooperative WNL, aiming to minimize the localization errors in the presence of network parameter uncertainty and transmitting power constraints. The main contributions of this work are as follows.

- We derive several tractable upper bounds for the localization performance metric, which involve only local network parameters;
- We propose distributed strategies for the robust power allocation, in which the underlying optimization problems are transformed into convex programs;
- We show the sparsity property of the optimal power allocation, leading to distributed sparsity-aided allocation strategies.

The rest of the paper is organized as follows. Section II presents the system model and then formulates the power allocation problem in the presence of network parameter uncertainty. Section III presents several important properties of the *individual* SPEB (iSPEB) in cooperative WNL. Section IV provides the design of distributed power allocation strategies. Section V shows the sparsity property of the optimal power allocation and presents the sparsity-aided allocation strategies. Finally, numerical results are presented in Section VI and conclusions are drawn in the last section.

Notation: $[A]_{ij}$ denotes the element in the i^{th} row and j^{th} column of matrix A . \mathbf{I}_n denotes an $n \times n$ identity matrix. $\mathbf{0}_{m,n}$ denotes a $m \times n$ matrix with all 0's. $\mathbf{1}_n$ and $\mathbf{0}_n$ denote

n -dimensional vectors with all 1's and 0's, respectively. For $\mathbf{0}_{m,n}$, $\mathbf{1}_n$, and $\mathbf{0}_n$, the subscript will be omitted if clear in the context. \mathbf{e}_k is a unit vector with the k^{th} element being 1 and all other elements being 0's. $\|\cdot\|_0$ denotes the number of non-zero elements. The operation \otimes denotes the Kronecker product. Matrix $\mathbf{J}_r(\phi)$ is defined as $\mathbf{J}_r(\phi) = [\cos \phi \ \sin \phi]^T [\cos \phi \ \sin \phi]$. For vectors \mathbf{x} and \mathbf{y} , the relations $\mathbf{x} \succeq \mathbf{y}$ and $\mathbf{x} \succ \mathbf{y}$ denote that all elements of $\mathbf{x} - \mathbf{y}$ are nonnegative and positive, respectively. For square matrices \mathbf{A} and \mathbf{B} , the relation $\mathbf{A} \succeq \mathbf{B}$ denotes that $\mathbf{A} - \mathbf{B}$ is a semidefinite matrix.

II. PROBLEM FORMULATION

This section introduces the system model for cooperative WNL and formulates the distributed power allocation problems. The uncertainty model for network parameters is also presented, which leads to robust formulations.

A. System Model

Consider a two-dimensional synchronized wireless network with N_b anchors and N_a agents. Anchors, with known positions, constitute infrastructure such as cellular base stations. Agents are mobile devices with unknown positions. Let $\mathcal{N}_a = \{1, 2, \dots, N_a\}$ denote the set of agents and $\mathcal{N}_b = \{N_a+1, N_a+2, \dots, N_a+N_b\}$ denote the set of anchors. The position of node k is denoted by a vector \mathbf{p}_k , and the angle and the distance from node j to node k is denoted by ϕ_{kj} and d_{kj} , respectively. The unknown positions of the agents are written in a vector form $\mathbf{p} = [\mathbf{p}_1^T \ \mathbf{p}_2^T \ \dots \ \mathbf{p}_{N_a}^T]^T$.

In cooperative WNL, each agent aims to determine its position based on the range measurements to neighboring agents as well as to neighboring anchors. In particular, two kinds of transmission for localization are considered:

- Anchor transmission (infrastructure): anchor j transmits a ranging signal to agent k with power x_{kj} ;
- Agent transmission (cooperation): agent j transmits a ranging signal to agent k with power x_{kj} .

Let $\{x_{kj}\}_{k \in \mathcal{N}_a, j \in \mathcal{N}_a \cup \mathcal{N}_b}$ denote the *power allocation set*, for which the shorthand $\{x_{kj}\}$ will be used in the rest of the paper unless otherwise specified.

B. Distributed Power Allocation Formulation

The performance metrics for cooperative WNL are presented as follows. Let $\mathbf{J}_e(\mathbf{p})$ denote the *network* equivalent Fisher information matrix (EFIM) given by (1) at the bottom of next page, where $\mathbf{J}_e^A(\mathbf{p}_k)$ and \mathbf{C}_{kj} are given by

$$\mathbf{J}_e^A(\mathbf{p}_k) = \sum_{j \in \mathcal{N}_b} x_{kj} \xi_{kj} \mathbf{J}_r(\phi_{kj})$$

and

$$\mathbf{C}_{kj} = (x_{kj} \xi_{kj} + x_{jk} \xi_{jk}) \mathbf{J}_r(\phi_{kj})$$

respectively [25].² In the above expressions, ξ_{kj} is the equivalent ranging coefficient (ERC) that depends on the channel condition between node k and j [35]. Note that by

²For notational convenience, the dependence of the power allocation set on $\mathbf{J}_e(\mathbf{p})$ are suppressed throughout the paper.

simply setting $\xi_{kj} = \xi_{jk} = 0$, the EFIM given by (1) can be specialized to networks in which nodes k and j are not connected.

For $k \in \mathcal{N}_a$, let $\hat{\mathbf{p}}_k$ be an unbiased estimator of \mathbf{p}_k . It is shown that the mean squared error for $\hat{\mathbf{p}}_k$ is lower bounded by the iSPEB $\mathcal{P}(\mathbf{p}_k)$, i.e.,

$$\mathbb{E}\{\|\hat{\mathbf{p}}_k - \mathbf{p}_k\|^2\} \geq \mathcal{P}(\mathbf{p}_k) := \text{tr}\{\mathbf{J}_e^{-1}(\mathbf{p}_k)\} \quad (2)$$

where the *individual* EFIM $\mathbf{J}_e(\mathbf{p}_k)$ is a 2×2 matrix that retains all the necessary information to derive the information inequality for the parameter \mathbf{p}_k [25].³

The iSPEB is adopted as a performance metric, and the goal of distributed power allocation is to achieve the minimum iSPEB by allocating transmitting power \mathbf{x}_k associated with agent k , where \mathbf{x}_k is the vector consisting of $\{x_{kj}\}_{j \in \mathcal{N}_b} \cup \{x_{jk}\}_{j \in \mathcal{N}_a \setminus \{k\}}$. Such a problem can be formulated as

$$\begin{aligned} \mathcal{P}_k : \quad & \min_{\mathbf{x}_k} \quad \mathcal{P}(\mathbf{p}_k) \\ & \text{s.t.} \quad \sum_{j \in \mathcal{N}_b} x_{kj} \leq P_{\text{anc}}^{(k)} \end{aligned} \quad (3)$$

$$\sum_{j \in \mathcal{N}_a \setminus \{k\}} x_{jk} \leq P_{\text{agt}}^{(k)} \quad (4)$$

$$\mathbf{x}_k \succeq \mathbf{0} \quad (5)$$

where $P_{\text{anc}}^{(k)}$ and $P_{\text{agt}}^{(k)}$ are the total power associated with agent k for anchor transmission and agent transmission, respectively.

Remark 1: The above formulation reduces to the non-cooperative case by setting $x_{kj} = 0$ for all $k \in \mathcal{N}_a$ and $j \in \mathcal{N}_a$ in the constraints.

C. Uncertainty Model and Robust Formulation

Perfect estimates of network parameters (angles and ERCs) are often unavailable in practice; for example, the angles depend on agents' positions, which need to be inferred in WNL. This motivates the robust formulation of power allocation problems, where the design of strategies accounts for the uncertainty associated with the estimated parameters.⁴ The goal of robust power allocation is to minimize the iSPEB subject to power constraints and network parameter uncertainty.

For agent k and node j , let $\hat{\phi}_{kj}$ and $\hat{\xi}_{kj}$ denote the nominal values of the angle ϕ_{kj} and ERC ξ_{kj} , respectively. Consider

³The SPEB is obtained via information inequality and is asymptotically achievable by the maximum likelihood estimators in high SNR regimes [40]–[42]. High-accuracy WNL systems often operate in such regimes via the use of repeated transmissions, coded sequences, or spread spectrum techniques, etc.

⁴For example, in applications such as navigation and tracking, the estimated parameters can be obtained from previous time steps.

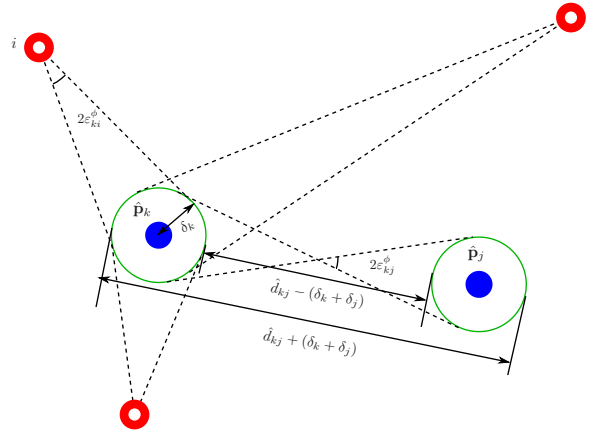


Fig. 2. Example of the uncertainty model: each agent is located in one of the green circles; for agent k , the circle is centered at $\hat{\mathbf{p}}_k$ with radius δ_k .

that the actual parameters lie in the linear sets

$$\phi_{kj} \in [\hat{\phi}_{kj} - \varepsilon_{kj}^\phi, \hat{\phi}_{kj} + \varepsilon_{kj}^\phi] =: \mathcal{S}_{kj}^\phi \quad (6)$$

$$\xi_{kj} \in [\hat{\xi}_{kj} - \varepsilon_{kj}^\xi, \hat{\xi}_{kj} + \varepsilon_{kj}^\xi] =: \mathcal{S}_{kj}^\xi \quad (7)$$

where ε_{kj}^ϕ and ε_{kj}^ξ are positive scalars denoting the maximum uncertainty. Fig. 2 provides an example of the uncertainty model. Agent k is located in a circle centered at $\hat{\mathbf{p}}_k$ with radius δ_k . In this case, $\varepsilon_{kj}^\phi = \arcsin((\delta_k + \delta_j)/\hat{d}_{kj})$, where \hat{d}_{kj} is the estimate of the distance between agent k and agent j .

The worst-case iSPEB for agent k due to the network parameter uncertainty (6) and (7) is given by

$$\mathcal{P}_R(\mathbf{p}_k) := \max_{\{\phi_{kj} \in \mathcal{S}_{kj}^\phi, \xi_{kj} \in \mathcal{S}_{kj}^\xi\}} \mathcal{P}(\mathbf{p}_k) \quad (8)$$

and correspondingly, the robust power allocation problem is given by

$$\begin{aligned} \mathcal{P}_{k-R} : \quad & \min_{\mathbf{x}_k} \quad \mathcal{P}_R(\mathbf{p}_k) \\ & \text{s.t.} \quad (3) - (5). \end{aligned}$$

Remark 2: When the parameter uncertainty vanishes, the worst-case iSPEB $\mathcal{P}_R(\mathbf{p}_k)$ reduces to $\mathcal{P}(\mathbf{p}_k)$ and consequently, the robust power allocation problem \mathcal{P}_{k-R} reduces to the non-robust problem \mathcal{P}_k .

III. PROPERTIES OF SPEB

This section presents several important properties of the iSPEB and lower bounds on the individual EFIM.

$$\mathbf{J}_e(\mathbf{p}) = \begin{bmatrix} \mathbf{J}_e^A(\mathbf{p}_1) + \sum_{j \in \mathcal{N}_a \setminus \{1\}} \mathbf{C}_{1,j} & -\mathbf{C}_{1,2} & \cdots & -\mathbf{C}_{1,N_a} \\ -\mathbf{C}_{2,1} & \mathbf{J}_e^A(\mathbf{p}_2) + \sum_{j \in \mathcal{N}_a \setminus \{2\}} \mathbf{C}_{2,j} & & -\mathbf{C}_{2,N_a} \\ \vdots & & \ddots & \\ -\mathbf{C}_{N_a,1} & -\mathbf{C}_{N_a,2} & & \mathbf{J}_e^A(\mathbf{p}_{N_a}) + \sum_{j \in \mathcal{N}_a \setminus \{N_a\}} \mathbf{C}_{N_a,j} \end{bmatrix} \quad (1)$$

A. SPEB Properties

The network EFIM $\mathbf{J}_e(\mathbf{p})$ can be written as a linear combination of positive semidefinite matrices, given by

$$\mathbf{J}_e(\mathbf{p}) = \sum_{k \in \mathcal{N}_a} \sum_{j \in \mathcal{N}_a \cup \mathcal{N}_b \setminus \{k\}} x_{kj} \xi_{kj} \mathbf{u}_{kj} \mathbf{u}_{kj}^T$$

where $\mathbf{u}_{kj} \in \mathbb{R}^{2N_a}$ is given by

$$\mathbf{u}_{kj} = \begin{cases} \mathbf{e}_k \otimes [\cos \phi_{kj} & \sin \phi_{kj}]^T & \text{if } j \in \mathcal{N}_b \\ (\mathbf{e}_k - \mathbf{e}_j) \otimes [\cos \phi_{kj} & \sin \phi_{kj}]^T & \text{if } j \in \mathcal{N}_a \end{cases}$$

in which \mathbf{e}_k and \mathbf{e}_j are N_a -dimensional vectors. Using this expression of network EFIM, the following properties of the iSPEB can be obtained.

Proposition 1 (Convexity): The iSPEB $\mathcal{P}(\mathbf{p}_k)$ is convex in \mathbf{x}_k .

Proof: See Appendix A. \square

Proposition 1 implies that \mathcal{P}_k is a convex program since the objective function is convex and the constraints are linear. Thus, the optimal solution for \mathcal{P}_k can be obtained using standard convex optimization algorithms provided that the power allocation vectors of other agents, i.e., $\{\mathbf{x}_j\}_{j \in \mathcal{N}_a \setminus \{k\}}$, are available.

Proposition 2 (Monotonicity): The iSPEB $\mathcal{P}(\mathbf{p}_k)$ is non-increasing in power allocation vector \mathbf{x}_k .

Proof: See Appendix B. \square

Proposition 2 implies that the iSPEB is monotonically non-increasing in ξ_{kj} , and thus the maximization over ξ_{kj} to obtain the worst-case iSPEB is straightforward:

$$\mathcal{P}_R(\mathbf{p}_k) = \max_{\{\phi_{kj} \in \mathcal{S}_{kj}^\phi, \xi_{kj} = \underline{\xi}_{kj}\}} \mathcal{P}(\mathbf{p}_k)$$

where $\underline{\xi}_{kj} = \hat{\xi}_{kj} - \varepsilon_{kj}^\xi$.

Note that the optimal solutions of \mathcal{P}_k 's and \mathcal{P}_{k-R} cannot be obtained in a distributed manner because the iSPEBs $\mathcal{P}(\mathbf{p}_k)$ and $\mathcal{P}_R(\mathbf{p}_k)$ depend on the angles and ERCs of the entire network as well as the power allocation vectors of other agents. Hence, we will derive upper bounds for $\mathcal{P}(\mathbf{p}_k)$ and $\mathcal{P}_R(\mathbf{p}_k)$ that are amenable for distributed implementation in Section III-B and Section III-C, respectively.

B. Upper Bounds for Distributed Implementation

This section provides upper bounds for the iSPEB $\mathcal{P}(\mathbf{p}_k)$, involving only the local network parameters. Consider the following two auxiliary matrices:

$$\mathbf{J}_e^I(\mathbf{p}_k) = \mathbf{J}_e^A(\mathbf{p}_k) + \sum_{j \in \mathcal{N}_a \setminus \{k\}} \frac{x_{jk} \xi_{jk} \mathbf{J}_r(\phi_{jk})}{1 + x_{jk} \xi_{jk} \Delta_{jk}} \quad (9)$$

$$\mathbf{J}_e^{II}(\mathbf{p}_k) = \mathbf{J}_e^A(\mathbf{p}_k) + \sum_{j \in \mathcal{N}_a \setminus \{k\}} \frac{x_{jk} \xi_{jk} \mathbf{J}_r(\phi_{jk})}{1 + P_{\text{agt}}^{(k)} \xi_{jk} \Delta_{jk}} \quad (10)$$

where

$$\Delta_{jk} = \mathbf{v}_{jk}^T [\mathbf{J}_e^A(\mathbf{p}_k)]^{-1} \mathbf{v}_{jk}$$

in which $\mathbf{v}_{jk} = [\cos \phi_{jk} \quad \sin \phi_{jk}]^T$.⁵ The next proposition shows that these auxiliary matrices are lower bounds for $\mathbf{J}_e(\mathbf{p}_k)$.

Proposition 3: The EFIM for agent k is bounded as

$$\mathbf{J}_e^{II}(\mathbf{p}_k) \preceq \mathbf{J}_e^I(\mathbf{p}_k) \preceq \mathbf{J}_e(\mathbf{p}_k).$$

Proof: See Appendix C. \square

Proposition 3 implies that

$$\mathcal{P}(\mathbf{p}_k) \leq \mathcal{P}^I(\mathbf{p}_k) \leq \mathcal{P}^{II}(\mathbf{p}_k)$$

where

$$\mathcal{P}^I(\mathbf{p}_k) = \text{tr} \left\{ [\mathbf{J}_e^I(\mathbf{p}_k)]^{-1} \right\}$$

$$\mathcal{P}^{II}(\mathbf{p}_k) = \text{tr} \left\{ [\mathbf{J}_e^{II}(\mathbf{p}_k)]^{-1} \right\}$$

are upper bounds for the iSPEB of agent k . Note that if Δ_{jk} is available,⁶ then $\mathbf{J}_e^I(\mathbf{p}_k)$ and $\mathbf{J}_e^{II}(\mathbf{p}_k)$ depend only on local network parameters and power allocation vectors of agent k ; that is, they do not rely on the parameters of the entire network or the power allocation vectors of other agents. Therefore, these bounds for the iSPEB are amenable for distributed power allocation. In addition, since $\mathcal{P}^I(\mathbf{p}_k)$ and $\mathcal{P}^{II}(\mathbf{p}_k)$ are upper bounds for the iSPEB, the power allocation programs that adopt them as the objective functions are conservative relaxations and their solutions will result in localization errors small than the corresponding objective values.

Note that the denominator in the summand of the expression in right-hand side of (10) does not contain x_{jk} . Therefore, the EFIM $\mathbf{J}_e^{II}(\mathbf{p}_k)$ is linear in x_{jk} , and such a linear form will permit more efficient optimization, e.g., SDP [34]. Indeed, this form of EFIM will permit even more efficient convex optimization, e.g., SOCP [35].

C. Upper bounds with Parameter Uncertainty

This section provides upper bounds for the worst-case iSPEB $\mathcal{P}_R(\mathbf{p}_k)$ in the presence of network parameter uncertainty. Consider the following matrix

$$\mathbf{Q}_e^A(\mathbf{p}_k) := \sum_{j \in \mathcal{N}_b} x_{kj} \underline{\xi}_{kj} (\mathbf{J}_r(\hat{\phi}_{kj}) - \delta_{kj} \mathbf{I})$$

where $\delta_{kj} = |\sin \varepsilon_{kj}^\phi|$. Then it can be shown that for any $\phi_{kj} \in \mathcal{S}_{kj}^\phi$ and $\xi_{kj} \in \mathcal{S}_{kj}^\xi$,

$$\mathbf{Q}_e^A(\mathbf{p}_k) \preceq \mathbf{J}_e^A(\mathbf{p}_k)$$

and consequently,

$$\mathcal{P}^A(\mathbf{p}_k) := \text{tr} \left\{ [\mathbf{J}_e^A(\mathbf{p}_k)]^{-1} \right\} \leq \text{tr} \left\{ [\mathbf{Q}_e^A(\mathbf{p}_k)]^{-1} \right\} \quad (11)$$

provided that $\mathbf{Q}_e^A(\mathbf{p}_k) \succeq 0$ [34].

Two additional auxiliary matrices are introduced as follows:

$$\mathbf{Q}_e^I(\mathbf{p}_k) = \mathbf{Q}_e^A(\mathbf{p}_k) + \sum_{j \in \mathcal{N}_a \setminus \{k\}} x_{jk} \chi_{jk}^I (\mathbf{J}_r(\hat{\phi}_{jk}) - \delta_{jk} \mathbf{I})$$

$$\mathbf{Q}_e^{II}(\mathbf{p}_k) = \mathbf{Q}_e^A(\mathbf{p}_k) + \sum_{j \in \mathcal{N}_a \setminus \{k\}} x_{jk} \chi_{jk}^{II} (\mathbf{J}_r(\hat{\phi}_{jk}) - \delta_{jk} \mathbf{I})$$

⁵In fact, Δ_{jk} is the directional position error bound of agent j (based solely on the anchors) along the angle ϕ_{jk} between the two agents [25].

⁶The knowledge of Δ_{jk} can be obtained by a sequential power allocation strategy, as discussed in Section IV.

where

$$\chi_{jk}^I = \frac{\xi_{jk}}{1 + x_{jk} \xi_{jk} \Delta_{jk}^R} \quad \text{and} \quad \chi_{jk}^{II} = \frac{\xi_{jk}}{1 + P_{\text{agt}}^{(k)} \xi_{jk} \Delta_{jk}^R}$$

in which

$$\Delta_{jk}^R = \max_{\phi_{jk} \in \mathcal{S}_{jk}^\phi} \mathbf{v}_{jk}^T [\mathbf{Q}_e^A(\mathbf{p}_j)]^{-1} \mathbf{v}_{jk}.$$

The next proposition shows that these two auxiliary matrices $\mathbf{Q}_e^I(\mathbf{p}_k)$ and $\mathbf{Q}_e^{II}(\mathbf{p}_k)$ are lower bounds of $\mathbf{J}_e^I(\mathbf{p}_k)$ and $\mathbf{J}_e^{II}(\mathbf{p}_k)$, respectively.

Proposition 4: Under the uncertainty model (6) and (7),

$$\begin{aligned} \mathbf{Q}_e^I(\mathbf{p}_k) &\preceq \mathbf{J}_e^I(\mathbf{p}_k), & \forall \phi_{kj} \in \mathcal{S}_{kj}^\phi, \xi_{kj} \in \mathcal{S}_{kj}^\xi \\ \mathbf{Q}_e^{II}(\mathbf{p}_k) &\preceq \mathbf{J}_e^{II}(\mathbf{p}_k), & \forall \phi_{kj} \in \mathcal{S}_{kj}^\phi, \xi_{kj} \in \mathcal{S}_{kj}^\xi \end{aligned}$$

provided that $\mathbf{Q}_e^A(\mathbf{p}_k) \succeq 0$.

Proof: Note that

$$\begin{aligned} \Delta_{jk}^R &\geq \mathbf{v}_{jk}^T [\mathbf{Q}_e^A(\mathbf{p}_k)]^{-1} \mathbf{v}_{jk} \\ &\geq \mathbf{v}_{jk}^T [\mathbf{J}_e^A(\mathbf{p}_k)]^{-1} \mathbf{v}_{jk} = \Delta_{jk} \end{aligned}$$

where the first inequality is due to the definition of Δ_{jk}^R and the second inequality is due to $\mathbf{J}_e^A(\mathbf{p}_k) \succeq \mathbf{Q}_e^A(\mathbf{p}_k)$ and $\mathbf{Q}_e^A(\mathbf{p}_k) \succeq 0$. Thus one can obtain

$$\begin{aligned} \chi_{jk}^I &= \frac{\xi_{jk}}{1 + x_{jk} \xi_{jk} \Delta_{jk}^R} \leq \frac{\xi_{jk}}{1 + x_{jk} \xi_{jk} \Delta_{jk}} \\ &\leq \frac{\xi_{jk}}{1 + x_{jk} \xi_{jk} \Delta_{jk}} \end{aligned}$$

and similarly

$$\chi_{jk}^{II} \leq \frac{\xi_{jk}}{1 + P_{\text{agt}}^{(k)} \xi_{jk} \Delta_{jk}}.$$

Moreover, note that $\mathbf{Q}_e^A(\mathbf{p}_k) \preceq \mathbf{J}_e^A(\mathbf{p}_k)$ and $(\mathbf{J}_r(\hat{\phi}_{jk}) - \delta_{jk} \mathbf{I}) \preceq \mathbf{J}_r(\phi_{jk})$ [34]. These inequalities lead to the claim of the proposition. \square

Proposition 4 implies that for any $\phi_{kj} \in \mathcal{S}_{kj}^\phi$ and $\xi_{kj} \in \mathcal{S}_{kj}^\xi$,

$$\begin{aligned} \mathcal{P}^I(\mathbf{p}_k) &\leq \text{tr} \left\{ [\mathbf{Q}_e^I(\mathbf{p}_k)]^{-1} \right\} \\ \mathcal{P}^{II}(\mathbf{p}_k) &\leq \text{tr} \left\{ [\mathbf{Q}_e^{II}(\mathbf{p}_k)]^{-1} \right\} \end{aligned}$$

provided that $\mathbf{Q}_e^I(\mathbf{p}_k) \succeq 0$, $\mathbf{Q}_e^{II}(\mathbf{p}_k) \succeq 0$ and $\mathbf{Q}_e^A(\mathbf{p}_k) \succeq 0$. Consequently,

$$\mathcal{P}_R(\mathbf{p}_k) \leq \max_{\{\phi_{kj} \in \mathcal{S}_{kj}^\phi, \xi_{kj} \in \mathcal{S}_{kj}^\xi\}} \mathcal{P}^I(\mathbf{p}_k) \leq \text{tr} \left\{ [\mathbf{Q}_e^I(\mathbf{p}_k)]^{-1} \right\} \quad (12)$$

$$\mathcal{P}_R(\mathbf{p}_k) \leq \max_{\{\phi_{kj} \in \mathcal{S}_{kj}^\phi, \xi_{kj} \in \mathcal{S}_{kj}^\xi\}} \mathcal{P}^{II}(\mathbf{p}_k) \leq \text{tr} \left\{ [\mathbf{Q}_e^{II}(\mathbf{p}_k)]^{-1} \right\}. \quad (13)$$

Note that similarly to $\mathbf{J}_e^I(\mathbf{p}_k)$ and $\mathbf{J}_e^{II}(\mathbf{p}_k)$, if Δ_{jk}^R is available, then $\mathbf{Q}_e^I(\mathbf{p}_k)$ and $\mathbf{Q}_e^{II}(\mathbf{p}_k)$ depend only on local network parameters and power allocation vectors of agent k , facilitating the design of distributed power allocation strategies.

IV. DISTRIBUTED POWER ALLOCATION STRATEGIES

This section develops distributed power allocation strategies in the presence of network parameter uncertainty. These strategies also account for the non-robust cases in which the parameter uncertainty vanishes. In particular, the original problem is decomposed into infrastructure and cooperation phases, and distributed strategies are then designed for each phase.

A. Power Allocation Decomposition

Using the upper bound in (12) or (13) as the optimization objective for agent k requires the power allocation vectors of all other agents. Obtaining these vectors in turn require the power allocation vector of agent k in their optimization programs. To circumvent this difficulty, we transform the original problem into a sequential two-phase (infrastructure phase and cooperation phase) optimization problem and design distributed power allocation strategies for each phase. Specifically, each agent k accomplishes the tasks outlined as follows:

- infrastructure phase: determines the allocation of power transmitted from anchors to agent k and obtains its positional information;
- cooperation phase: determines the allocation of power transmitted from agent k to its neighboring agents, using their positional information obtained in the infrastructure phase.

The next two subsections will present the power allocation strategies in the infrastructure and cooperation phases.

B. Infrastructure Phase

For each agent k , $\mathcal{P}_R(\mathbf{p}_k)$ is minimized with respect to $\{x_{kj}\}_{j \in \mathcal{N}_b}$ with $x_{kj} = 0$ for all $j \in \mathcal{N}_a$. Using (11), the robust anchor power allocation problem for agent k can be formulated as

$$\begin{aligned} \mathcal{P}_{\text{anc}}^{(k)} : \quad & \min_{\{x_{kj}\}_{j \in \mathcal{N}_b}} \quad \text{tr} \left\{ [\mathbf{Q}_e^A(\mathbf{p}_k)]^{-1} \right\} \\ & \text{s.t.} \quad \mathbf{Q}_e^A(\mathbf{p}_k) \succeq 0 \end{aligned} \quad (3) \text{ and } (5).$$

This power allocation problem can be transformed into SDP by exploiting the properties of the SPEB as follows.

Proposition 5: Problem $\mathcal{P}_{\text{anc}}^{(k)}$ is equivalent to the SDP given by

$$\begin{aligned} \mathcal{P}_{\text{anc, SDP}}^{(k)} : \quad & \min_{\mathbf{M} \in \mathbb{R}^{2 \times 2}, \{x_{kj}\}_{j \in \mathcal{N}_b}} \quad \text{tr} \{ \mathbf{M} \} \\ & \text{s.t.} \quad \begin{bmatrix} \mathbf{M} & \mathbf{I} \\ \mathbf{I} & \mathbf{Q}_e^A(\mathbf{p}_k) \end{bmatrix} \succeq 0 \end{aligned} \quad (14) \quad (3) \text{ and } (5).$$

Proof: Consider adding a dummy constraint with an auxiliary matrix \mathbf{M} to $\mathcal{P}_{\text{anc}}^{(k)}$, resulting in

$$\begin{aligned} \mathcal{P}_{\text{anc, aux}}^{(k)} : \quad & \min_{\mathbf{M} \in \mathbb{R}^{2 \times 2}, \{x_{kj}\}_{j \in \mathcal{N}_b}} \quad \text{tr} \left\{ [\mathbf{Q}_e^A(\mathbf{p}_k)]^{-1} \right\} \\ & \text{s.t.} \quad \mathbf{Q}_e^A(\mathbf{p}_k) \succeq 0 \\ & \quad \mathbf{M} \succeq [\mathbf{Q}_e^A(\mathbf{p}_k)]^{-1} \end{aligned} \quad (15) \quad (3) \text{ and } (5)$$

which is equivalent to $\mathcal{P}_{\text{anc}}^{(k)}$. Note that (15), together with $\mathbf{Q}_e^A(\mathbf{p}_k) \succeq 0$, can be converted into (14) using the property of Schur complement. Moreover, note that (15) implies that

$$\text{tr}\{\mathbf{M}\} \geq \text{tr} \left\{ \left[\mathbf{Q}_e^A(\mathbf{p}_k) \right]^{-1} \right\}$$

and consequently, the objective function in $\mathcal{P}_{\text{anc,aux}}^{(k)}$ can be replaced by $\text{tr}\{\mathbf{M}\}$. Thus $\mathcal{P}_{\text{anc,SDP}}^{(k)}$ is equivalent to $\mathcal{P}_{\text{anc,aux}}^{(k)}$ and hence to $\mathcal{P}_{\text{anc}}^{(k)}$. Finally, since $\mathbf{Q}_e^A(\mathbf{p}_k)$ is linear in x_{kj} , $\mathcal{P}_{\text{anc,SDP}}^{(k)}$ is an SDP. \square

C. Cooperation Phase

Using the optimal solutions of $\mathcal{P}_{\text{anc}}^{(k)}$ in the infrastructure phase, each agent k obtains $\mathbf{Q}_e^A(\mathbf{p}_k)$ and transmits this to its neighbors. Then, the power allocation problems for agent k in the cooperation phase are formulated using (12) and (13) as relaxed performance metrics.

1) *Distributed Strategy I*: Based on (12), the power allocation problem for agent k in the cooperation phase is formulated as

$$\begin{aligned} \mathcal{P}_{\text{agt,I}}^{(k)} : \quad & \min_{\{x_{jk}\}_{j \in \mathcal{N}_a \setminus \{k\}}} \text{tr} \left\{ \left[\mathbf{Q}_e^I(\mathbf{p}_k) \right]^{-1} \right\} \\ \text{s.t.} \quad & \mathbf{Q}_e^I(\mathbf{p}_k) \succeq 0 \\ & (4) - (5). \end{aligned} \quad (16)$$

Note that $\mathcal{P}_{\text{agt,I}}^{(k)}$ is not necessarily a convex program since the feasible set corresponding to the constraint (16) may be nonconvex. To deal with this issue, consider the following problem

$$\begin{aligned} \mathcal{P}_{\text{aux,I}}^{(k)} : \quad & \min_{\mathbf{M} \in \mathbb{R}^{2 \times 2}, \{x_{jk}, y_j\}_{j \in \mathcal{N}_a \setminus \{k\}}} \text{tr}\{\mathbf{M}\} \\ \text{s.t.} \quad & \begin{bmatrix} \mathbf{M} & \mathbf{I} \\ \mathbf{I} & \tilde{\mathbf{Q}}_e^I(\mathbf{p}_k) \end{bmatrix} \succeq 0 \quad (17) \\ & 0 \leq y_j \leq \frac{x_{jk} \xi_{jk}}{1 + x_{jk} \xi_{jk} \Delta_{jk}^R}, \\ & j \in \mathcal{N}_a \setminus \{k\} \quad (18) \\ & (4) - (5) \end{aligned}$$

where

$$\tilde{\mathbf{Q}}_e^I(\mathbf{p}_k) = \mathbf{Q}_e^A(\mathbf{p}_k) + \sum_{j \in \mathcal{N}_a \setminus \{k\}} y_j (\mathbf{J}_r(\hat{\phi}_{jk}) - \delta_{jk} \mathbf{I}).$$

One can show that $\mathcal{P}_{\text{aux,I}}^{(k)}$ is a convex program since the feasible set corresponding to all the constraints is convex and the objective function is a linear function of the optimization variables. The next proposition shows that the optimal solution of $\mathcal{P}_{\text{agt,I}}^{(k)}$ can be obtained by solving the convex program $\mathcal{P}_{\text{aux,I}}^{(k)}$.

Proposition 6: The minimum objective value of $\mathcal{P}_{\text{agt,I}}^{(k)}$ is the same as that of $\mathcal{P}_{\text{aux,I}}^{(k)}$, and the optimal solution of $\mathcal{P}_{\text{agt,I}}^{(k)}$ can be obtained from that of $\mathcal{P}_{\text{aux,I}}^{(k)}$.

Proof: See Appendix D. \square

Algorithm 1 Distributed Power Allocation Strategies

Input: \mathcal{S}_{kj}^ϕ and \mathcal{S}_{kj}^ξ , $k \in \mathcal{N}_a$ and $j \in \mathcal{N}_a \cup \mathcal{N}_b \setminus \{k\}$

Output: $\{x_{kj}\}_{k \in \mathcal{N}_a, j \in \mathcal{N}_a \cup \mathcal{N}_b \setminus \{k\}}$

- 1: For $k \in \mathcal{N}_a$, agent k solves $\mathcal{P}_{\text{anc,SDP}}^{(k)}$ in the infrastructure phase
- 2: For $k \in \mathcal{N}_a$, agent k transmits $\mathbf{Q}_e^A(\mathbf{p}_k)$ to its neighboring agents
- 3: For $k \in \mathcal{N}_a$, agent k solves $\mathcal{P}_{\text{aux,I}}^{(k)}$ (or $\mathcal{P}_{\text{aux,II}}^{(k)}$) in the cooperation phase
- 4: Output x_{kj} .

2) *Distributed Strategy II*: Based on (13), the power allocation problem for agent k in the cooperation phase is formulated as

$$\begin{aligned} \mathcal{P}_{\text{agt,II}}^{(k)} : \quad & \min_{\{x_{jk}\}_{j \in \mathcal{N}_a \setminus \{k\}}} \text{tr} \left\{ \left[\mathbf{Q}_e^{II}(\mathbf{p}_k) \right]^{-1} \right\} \\ \text{s.t.} \quad & \mathbf{Q}_e^{II}(\mathbf{p}_k) \succeq 0 \\ & (4) - (5). \end{aligned}$$

As with Proposition 5, one can show that $\mathcal{P}_{\text{agt,II}}^{(k)}$ is equivalent to the following SDP.

$$\begin{aligned} \mathcal{P}_{\text{aux,II}}^{(k)} : \quad & \min_{\mathbf{M} \in \mathbb{R}^{2 \times 2}, \{x_{jk}\}_{j \in \mathcal{N}_a \setminus \{k\}}} \text{tr}\{\mathbf{M}\} \\ \text{s.t.} \quad & \begin{bmatrix} \mathbf{M} & \mathbf{I} \\ \mathbf{I} & \mathbf{Q}_e^{II}(\mathbf{p}_k) \end{bmatrix} \succeq 0 \\ & (4) - (5). \end{aligned}$$

Remark 3: Since $\mathcal{P}_{\text{aux,I}}^{(k)}$ and $\mathcal{P}_{\text{aux,II}}^{(k)}$ require only the estimates of the local network parameters, they are amenable for distributed implementation. The detailed power allocation strategies are described in Algorithm 1.

V. SPARSITY OF POWER ALLOCATION

This section first presents the sparsity property of the optimal power allocation and then proposes optimal anchor power allocation strategies based on the sparsity property for cooperative WNL. For ease of exposition, the strategy without parameter uncertainty is considered and the analysis for the robust case is analogous.

A. Sparsity of the Optimal Power Allocation Vector

Without loss of generality, the analysis focuses on the anchor power allocation for agent k (i.e., $\mathcal{P}_{\text{anc}}^{(k)}$) with the total power constraint $P_{\text{anc}}^{(k)} = 1$.

Let $\mathbf{y}_k = [x_{k(N_a+1)} \ x_{k(N_a+2)} \ \cdots \ x_{k(N_a+N_b)}]^T$ denote the anchor power allocation vector (APAV) for agent k . Then the objective function of $\mathcal{P}_{\text{anc}}^{(k)}$ can be written explicitly as follows [35]:

$$\mathcal{P}^A(\mathbf{p}_k; \mathbf{y}_k) = \frac{4 \cdot \mathbf{1}^T \mathbf{R}_k \mathbf{y}_k}{\mathbf{y}_k^T \mathbf{R}_k^T \mathbf{\Lambda}_k \mathbf{R}_k \mathbf{y}_k} \quad (19)$$

where $\mathbf{R}_k = \text{diag}\{\xi_{k(N_a+1)}, \xi_{k(N_a+2)}, \dots, \xi_{k(N_a+N_b)}\}$, and $\mathbf{\Lambda}_k \in \mathbb{R}^{N_b \times N_b}$ is a symmetric matrix,

$$\mathbf{\Lambda}_k = \mathbf{1}\mathbf{1}^T - \mathbf{c}_k \mathbf{c}_k^T - \mathbf{s}_k \mathbf{s}_k^T \quad (20)$$

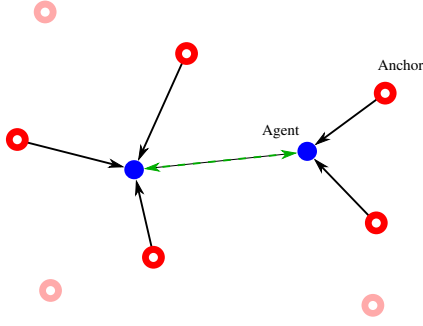


Fig. 3. Sparsity property of the optimal APAV: for each agent, the optimal localization accuracy can be achieved with at most three activated anchors.

with

$$\begin{aligned} \mathbf{c}_k &= [\cos \phi_{k(N_a+1)} \quad \cos \phi_{k(N_a+2)} \quad \cdots \quad \cos \phi_{k(N_a+N_b)}]^\top \\ \mathbf{s}_k &= [\sin \phi_{k(N_a+1)} \quad \sin \phi_{k(N_a+2)} \quad \cdots \quad \sin \phi_{k(N_a+N_b)}]^\top. \end{aligned}$$

Based on the expression of (19), the sparsity property of the optimal APAV will be given.

Proposition 7: There exists an optimal APAV \mathbf{y}_k^* for $\mathcal{P}_{\text{anc}}^{(k)}$ such that $\|\mathbf{y}_k^*\|_0 \leq \text{rank}\{\mathbf{\Lambda}_k\}$.

Proof: See Appendix E. \square

Remark 4: The matrix $\mathbf{\Lambda}_k$ in (20) is a linear combination of three rank-one symmetric matrices, implying that the rank of $\mathbf{\Lambda}_k$ is no more than three, i.e., $\text{rank}\{\mathbf{\Lambda}_k\} \leq 3$. Therefore, Proposition 7 implies the sparsity of the optimal APAV, i.e., each agent can achieve the optimal localization accuracy by activating at most three anchors. Fig. 3 illustrates the sparsity of the optimal APAV.

Since $\mathcal{P}_{\text{anc}}^{(k)}$ and $\mathcal{P}_{\text{agt,II}}^{(k)}$ have a similar structure, the sparsity property of the optimal power allocation also holds for $\mathcal{P}_{\text{agt,II}}^{(k)}$: each agent can achieve the optimal localization accuracy by making range measurements with at most three other agents. Such property enables us to develop sparsity-aided power allocation strategies. For brevity, the design of the strategy will focus on solving $\mathcal{P}_{\text{anc}}^{(k)}$ and the solution for $\mathcal{P}_{\text{agt,II}}^{(k)}$ can be obtained similarly.

B. Optimal Strategies for Simple Networks

Due to the sparsity of the APAV, the allocation strategy presented here will start from networks with three anchors, referred to as *simple networks*.

Proposition 8: For a simple network, if the following conditions hold

$$\begin{cases} \text{rank}\{\mathbf{\Lambda}_k\} = 3 \\ \mathbf{1}^\top (\mathbf{R}_k \mathbf{\Lambda}_k \mathbf{R}_k)^{-1} \mathbf{1} > 0 \\ (\mathbf{R}_k \mathbf{\Lambda}_k \mathbf{R}_k)^{-1} (\mathbf{R}_k \mathbf{1} + \alpha \mathbf{1}) \succ \mathbf{0} \end{cases} \quad (21)$$

where

$$\alpha = (\mathbf{1}^\top (\mathbf{R}_k \mathbf{\Lambda}_k \mathbf{R}_k)^{-1} \mathbf{1})^{-1/2}$$

then the unique optimal APAV for $\mathcal{P}_{\text{anc}}^{(k)}$ is given by

$$\mathbf{y}_k^* = \frac{A}{2\alpha} (\mathbf{R}_k \mathbf{\Lambda}_k \mathbf{R}_k)^{-1} (\mathbf{R}_k \mathbf{1} + \alpha \mathbf{1}) \quad (22)$$

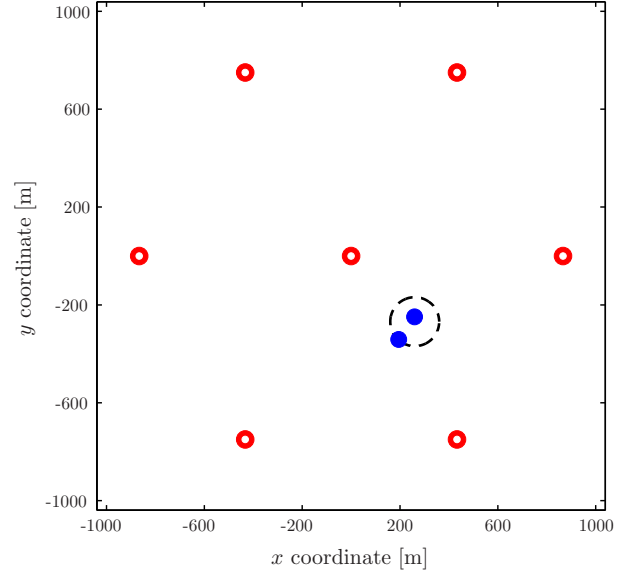


Fig. 4. The cooperative network consists of anchors (red circles) and agents (blue dots).

where

$$A = \frac{2\alpha}{\mathbf{1}^\top (\mathbf{R}_k \mathbf{\Lambda}_k \mathbf{R}_k)^{-1} (\mathbf{R}_k \mathbf{1} + \alpha \mathbf{1})}.$$

Otherwise, there exists an optimal APAV for $\mathcal{P}_{\text{anc}}^{(k)}$ with two positive elements and $\mathbf{y}_k^* = \tilde{\mathbf{y}}_k^{(i^*)}$, where

$$i^* = \arg \min_{i \in \{1,2,3\}} \mathcal{P}^A(\mathbf{p}_k; \tilde{\mathbf{y}}_k^{(i)})$$

in which

$$\begin{aligned} \tilde{\mathbf{y}}_k^{(1)} &= \frac{1}{a_2 + a_3} [0 \quad a_3 \quad a_2]^\top \\ \tilde{\mathbf{y}}_k^{(2)} &= \frac{1}{a_1 + a_3} [a_3 \quad 0 \quad a_1]^\top \\ \tilde{\mathbf{y}}_k^{(3)} &= \frac{1}{a_1 + a_2} [a_2 \quad a_1 \quad 0]^\top \end{aligned}$$

with $a_i = \sqrt{\xi_{k(N_a+i)}}$ for $i = 1, 2$ and 3.

Proof: See [43]. \square

Proposition 8 gives the power allocation strategy for $\mathcal{P}_{\text{anc}}^{(k)}$ in a closed form: if the conditions in (21) hold, the optimal APAV is given by (22); otherwise, the optimal APAV is the one (with the minimum objective value) of the three vectors.

The strategy in Proposition 8 can be extended to a general network with N_b anchors. There are $\binom{N_b}{3}$ distinct ways for selecting three anchors to form simple networks; then the optimal power allocation strategy is the one that corresponds to the simple network with the minimum SPEB. In small networks, this strategy is more efficient than SDP proposed in Section IV.

VI. NUMERICAL RESULTS

This section provides the performance evaluation of the proposed power allocation strategies, for which the convex optimization programs are solved by CVX [44].

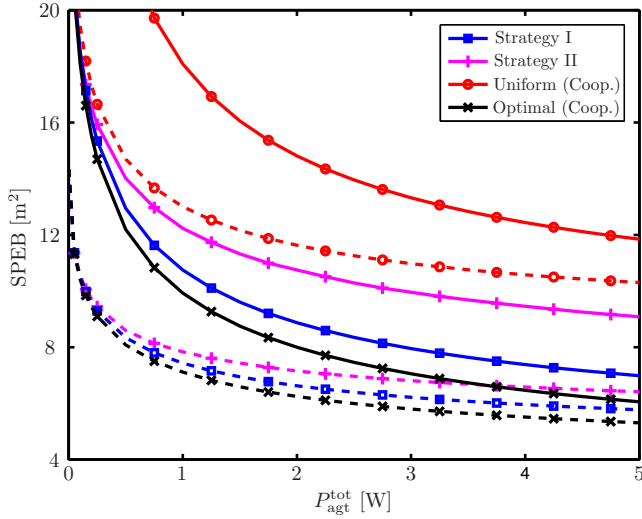


Fig. 5. Average SPEB with respect to $P_{\text{agt}}^{\text{tot}}$. Two cases for different N_a are considered: $N_a = 4$ (dashed lines) and $N_a = 8$ (solid lines).

Fig. 4 shows a two-dimensional cooperative network where seven anchors are placed in the vertices of equilateral triangles with circumradius of 500 meters. Agents are uniformly placed in a circular area with radius of 50 meters and the center of the circle is uniformly chosen in the whole $2000 \text{ m} \times 2000 \text{ m}$ area. Consider the ranging signals with carrier frequency $f_c = 2.1 \text{ GHz}$ and bandwidth $W = 40 \text{ MHz}$. The noise power density is -168 dBm/Hz . The WINNER channel model [45] is adopted for the ranging signal propagation as follows

$$\text{PL}[\text{dB}] = A + B \log_{10} d[\text{m}] + 20 \log_{10} \frac{f_c[\text{GHz}]}{5.0} + X$$

where $X \sim \mathcal{N}(0, \sigma^2)$ accounts for large-scale fading (i.e., shadowing). For anchor transmission, $A = 41.0$, $B = 23.8$, and $\sigma = 4$; for agent transmission, $A = 46.8$, $B = 18.7$, and $\sigma = 3$. The extended typical urban model is used for the power dispersion profile [46]. The ERCs ξ_{kj} are computed according to the formulas in [25]. The total transmitting power constraints in (3) and (4) are set to be the same for each agent, i.e., $P_{\text{anc}}^{(k)} = P_{\text{anc}}^{\text{tot}}/N_a$ and $P_{\text{agt}}^{(k)} = P_{\text{agt}}^{\text{tot}}/N_a$, where $P_{\text{anc}}^{\text{tot}} = 500 \text{ W}$ and $P_{\text{agt}}^{\text{tot}}$ takes specific values.

A. Localization Performance

This subsection evaluates the average SPEB for the following power allocation strategies in the absence of network parameter uncertainty:

- Strategy I described in Section IV-C1;
- Strategy II described in Section IV-C2;
- the uniform strategy, in which

$$\begin{aligned} x_{kj} &= P_{\text{anc}}^{(k)}/N_b, & j &\in \mathcal{N}_b \\ x_{jk} &= P_{\text{agt}}^{(k)}/(N_a - 1), & j &\in \mathcal{N}_a \setminus \{k\}; \end{aligned}$$

- the centralized strategy described in [47].

Fig. 5 shows the average SPEB as a function of the total agent transmitting power for all the four strategies where $N_a = 4$ and 8. It can be seen that for all the strategies, the

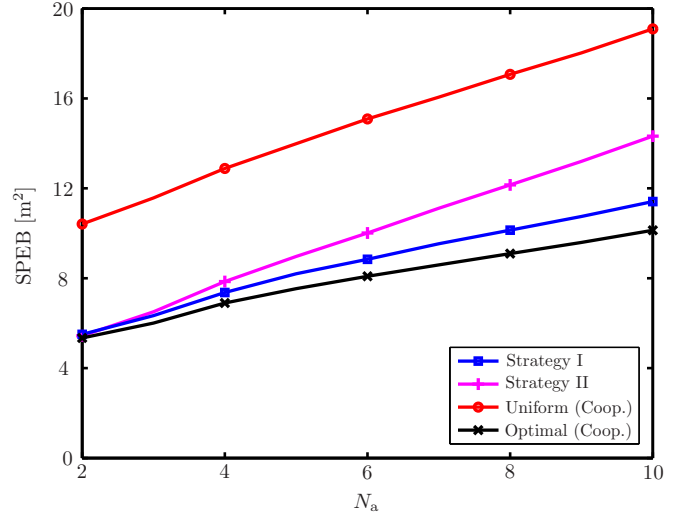


Fig. 6. Average SPEB with respect to the number of agents by different strategies for $P_{\text{agt}}^{\text{tot}} = 1.25 \text{ W}$.

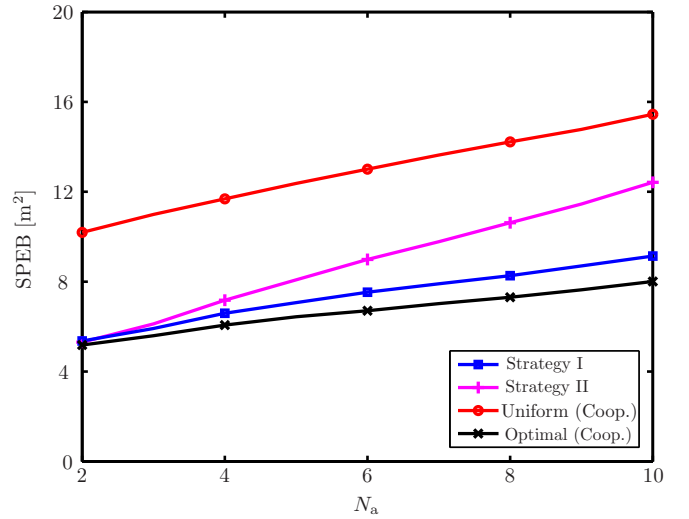


Fig. 7. Average SPEB with respect to the number of agents by different strategies for $P_{\text{agt}}^{\text{tot}} = 2.5 \text{ W}$.

average SPEB decreases with $P_{\text{agt}}^{\text{tot}}$ as the agents can better determine their positions with more transmitting power for their cooperation. Moreover, the SPEB decreases with $P_{\text{agt}}^{\text{tot}}$ at a slower rate for larger values of $P_{\text{agt}}^{\text{tot}}$, implying that the improvement of localization accuracy brought by the incremental transmitting power of cooperation diminishes when $P_{\text{agt}}^{\text{tot}}$ is large. These observations provide a guideline for the localization accuracy versus power consumption tradeoff.

Figs. 6 and 7 show the average SPEB as a function of the number of agents for all the four strategies where $P_{\text{agt}}^{\text{tot}} = 1.25 \text{ W}$ and 2.5 W , respectively. It can be seen that Strategies I and II significantly outperform the uniform strategy. For example when $N_a = 6$ and $P_{\text{agt}}^{\text{tot}} = 1.25 \text{ W}$, both strategies reduce the average SPEB by more than 30% compared to the uniform strategy. Moreover, Strategy I performs better than Strategy II, especially for large N_a , since the former adopts a tighter bound for the SPEB as the objective function.

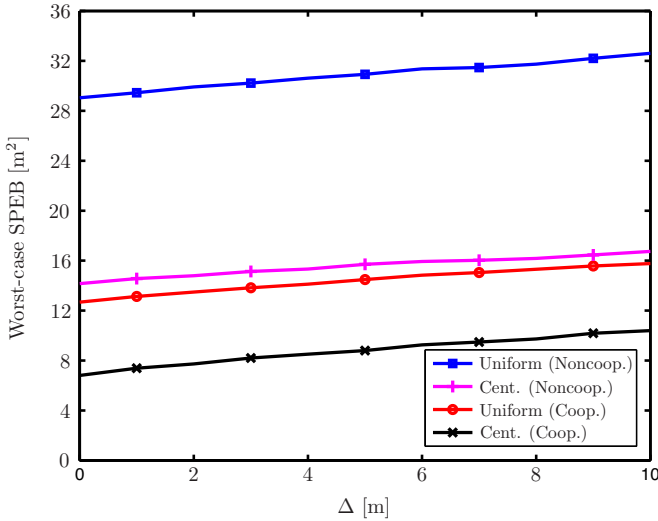


Fig. 8. Worst-case SPEB with respect to USS by the centralized strategy and the uniform strategy. In the cooperation setting, $P_{\text{agt}}^{\text{tot}} = 1.25$ W.

Finally, the performance loss of Strategies I and II compared to the optimal centralized strategy increases with the number of agents. This can be attributed to the fact that the bounds for the SPEB used in the proposed strategies are tighter in smaller networks.

B. Effects of Network Parameter Uncertainty

This subsection evaluates the worst-case SPEB for the robust power allocation strategies in the presence of network parameter uncertainty. Consider a network with four agents, in which the uncertainty region of each agent is a circle with radius Δ , referred to as the USS. Thus, for agent k , $\varepsilon_{k,j}^{\phi} = \arcsin(\Delta/\hat{d}_{k,j})$ for $j \in \mathcal{N}_b$, while $\varepsilon_{k,j}^{\phi} = 2 \arcsin(\Delta/\hat{d}_{k,j})$ for $j \in \mathcal{N}_a \setminus \{k\}$.

Fig. 8 shows the worst-case SPEB as a function of the USS for the centralized and uniform strategies where $P_{\text{agt}}^{\text{tot}} = 0$ W (non-cooperative setting) and $P_{\text{agt}}^{\text{tot}} = 1.25$ W (cooperative setting).⁷ It can be seen that the worst-case SPEB increases with the USS. This is because larger USS translates into a larger range of network parameters and consequently a larger worst-case SPEB. Moreover, the centralized strategy significantly outperform the uniform strategy in both settings. For example, in the cooperative setting, the centralized strategy reduces the worst-case SPEB by more than 34% compared to the uniform strategy. Finally, both strategies perform better in the cooperative setting than in the non-cooperative setting.

Fig. 9 shows the worst-case SPEB as a function of the USS for all the four strategies where $P_{\text{agt}}^{\text{tot}} = 1.25$ W. It can be seen that the worst-case SPEB increases with the USS for all the strategies as with Fig. 8. Moreover, Strategies I and II have almost the identical performance and both outperform the uniform strategy, reducing the worst-case SPEB by more than 36%. Finally, the performance loss of Strategies I and II

⁷The centralized strategy for the robust case can be obtained by extending that for the non-robust case developed in [47] using a similar technique proposed in Section III-C.

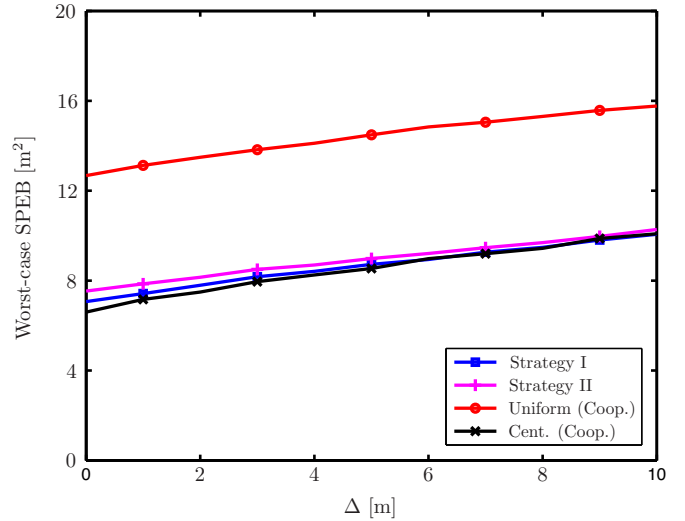


Fig. 9. Worst-case SPEB with respect to USS by proposed strategies, the uniform strategy and the centralized strategy.

compared to the centralized strategy is no greater than 7%, showing the near-optimality and the robustness provided by the two proposed distributed strategies.

VII. CONCLUSION

In this paper, we established an optimization framework for robust power allocation in cooperative WNL. Based on such framework, we developed efficient and distributed power allocation strategies via relaxation methods. We also discovered the sparsity property of optimal power allocation for WNL, leading to more efficient power allocation strategies in cooperative networks. The simulation results showed that the proposed power allocation strategies significantly outperform the uniform ones and achieve near-optimal performance. The outcome of this paper provides a guideline for the design of practical power allocation strategies, enabling robust and energy-efficient localization networks.

APPENDIX A PROOF OF PROPOSITION 1

Note that if $\mathbf{X} \succeq 0$, $[\mathbf{X}^{-1}]_{2k-1,2k-1}$ and $[\mathbf{X}^{-1}]_{2k,2k}$ are convex and non-increasing functions in \mathbf{X} [48, p. 110]. In addition, $\mathbf{J}_e(\mathbf{p})$ is a linear function of \mathbf{x}_k . By the convexity property of the composition functions [48, p. 86], $\mathcal{P}(\mathbf{p}_k)$ is a convex function in \mathbf{x}_k .

APPENDIX B PROOF OF PROPOSITION 2

For two power allocation vectors \mathbf{x}_k and \mathbf{y}_k , suppose $\mathbf{x}_k \succeq \mathbf{y}_k$ and let $\{x_{ij}\}$ and $\{y_{ij}\}$ denote the corresponding power allocation sets such that $\mathbf{x}_i = \mathbf{y}_i$ for $i \in \mathcal{N}_a \setminus \{k\}$. Then, the difference between the EFIMs associated with power

allocation sets $\{x_{ij}\}$ and $\{y_{ij}\}$ is given by

$$\begin{aligned} & \mathbf{J}_e(\mathbf{p}; \{x_{ij}\}) - \mathbf{J}_e(\mathbf{p}; \{y_{ij}\}) \\ &= \sum_{i \in \mathcal{N}_a} \sum_{j \in \mathcal{N}_a \cup \mathcal{N}_b \setminus \{i\}} (x_{ij} - y_{ij}) \xi_{ij} \mathbf{u}_{ij} \mathbf{u}_{ij}^T \\ &= \sum_{j \in \mathcal{N}_b} (x_{kj} - y_{kj}) \xi_{kj} \mathbf{u}_{kj} \mathbf{u}_{kj}^T \\ &+ \sum_{j \in \mathcal{N}_a \setminus \{k\}} (x_{jk} - y_{jk}) \xi_{jk} \mathbf{u}_{jk} \mathbf{u}_{jk}^T \end{aligned}$$

where the last equality is due to the fact that $\mathbf{x}_i = \mathbf{y}_i$ for $i \in \mathcal{N}_a \setminus \{k\}$. Note that $x_{kj} - y_{kj} \geq 0$, $\xi_{kj} \geq 0$, and $\mathbf{u}_{kj} \mathbf{u}_{kj}^T$ are positive semidefinite matrices. Therefore,

$$\mathbf{J}_e(\mathbf{p}; \{x_{ij}\}) - \mathbf{J}_e(\mathbf{p}; \{y_{ij}\}) \succeq \mathbf{0}$$

and hence $\mathbf{J}_e^{-1}(\mathbf{p}; \{x_{ij}\}) \preceq \mathbf{J}_e^{-1}(\mathbf{p}; \{y_{ij}\})$, which leads to the claim

$$\text{tr} \left\{ \left[\mathbf{J}_e^{-1}(\mathbf{p}; \{x_{ij}\}) \right]_{\mathbf{p}_k} \right\} \leq \text{tr} \left\{ \left[\mathbf{J}_e^{-1}(\mathbf{p}; \{y_{ij}\}) \right]_{\mathbf{p}_k} \right\}.$$

where $[\mathbf{J}_e^{-1}(\mathbf{p})]_{\mathbf{p}_k}$ denotes the square submatrix on the diagonal of $\mathbf{J}_e^{-1}(\mathbf{p})$ corresponding to \mathbf{p}_k .

APPENDIX C PROOF OF PROPOSITION 3

Without loss of generality, the proof focuses on the first agent. Consider $\mathbf{J}_e^L(\mathbf{p})$, representing the EFIM ignoring the cooperation among agents in $\mathcal{N}_a \setminus \{1\}$, in (23) shown at the bottom of this page. Note that $\mathbf{J}_e^L(\mathbf{p}) \preceq \mathbf{J}_e(\mathbf{p})$ since

$$\begin{aligned} & \mathbf{J}_e(\mathbf{p}) - \mathbf{J}_e^L(\mathbf{p}) \\ &= \frac{1}{2} \sum_{k \in \mathcal{N}_a \setminus \{1\}} \sum_{j \in \mathcal{N}_a \setminus \{1, k\}} (x_{jk} \xi_{jk} + x_{kj} \xi_{kj}) \mathbf{u}_{kj} \mathbf{u}_{kj}^T \succeq \mathbf{0} \end{aligned}$$

where the inequality is due to the fact that each summand is positive semidefinite. Consequently,

$$\mathbf{J}_e(\mathbf{p}_1) \succeq \mathbf{J}_e^L(\mathbf{p}_1). \quad (24)$$

The EFIM for agent 1 based on $\mathbf{J}_e^L(\mathbf{p})$ is given as

$$\begin{aligned} & \mathbf{J}_e^L(\mathbf{p}_1) \\ &= \mathbf{J}_e^A(\mathbf{p}_1) + \sum_{j \in \mathcal{N}_a \setminus \{1\}} \left[\mathbf{C}_{1,j} - \mathbf{C}_{1,j} (\mathbf{J}_e^A(\mathbf{p}_j) + \mathbf{C}_{j,1})^{-1} \mathbf{C}_{j,1} \right] \end{aligned} \quad (25)$$

$$\stackrel{(a)}{=} \mathbf{J}_e^A(\mathbf{p}_1) + \sum_{j \in \mathcal{N}_a \setminus \{1\}} \frac{(x_{1j} \xi_{1j} + x_{j1} \xi_{j1}) \mathbf{J}_r(\phi_{1j})}{1 + (x_{1j} \xi_{1j} + x_{j1} \xi_{j1}) \Delta_{j1}}$$

$$\stackrel{(b)}{\succeq} \mathbf{J}_e^A(\mathbf{p}_1) + \sum_{j \in \mathcal{N}_a \setminus \{1\}} \frac{x_{j1} \xi_{j1} \mathbf{J}_r(\phi_{j1})}{1 + x_{j1} \xi_{j1} \Delta_{j1}} = \mathbf{J}_e^L(\mathbf{p}_1) \quad (26)$$

where (a) can be verified after some algebra by noting

$$\mathbf{C}_{1,j} = (x_{1j} \xi_{1j} + x_{j1} \xi_{j1}) \mathbf{v}_{1j} \mathbf{v}_{1j}^T$$

and (b) holds since $\mathbf{J}_r(\phi_{1j}) \succeq \mathbf{0}$ and $y/(1+y\Delta_{j1})$ increases in y . Equations (24) and (26) give the result $\mathbf{J}_e(\mathbf{p}_1) \succeq \mathbf{J}_e^L(\mathbf{p}_1) \succeq \mathbf{J}_e^L(\mathbf{p}_1)$.

Moreover, due to the power constraints for the agent transmission, it follows that $x_{jk} \leq P_{\text{agt}}^{(k)}$ and hence

$$\frac{\xi_{jk}}{1 + P_{\text{agt}}^{(k)} \xi_{jk} \Delta_{jk}} \leq \frac{\xi_{jk}}{1 + x_{jk} \xi_{jk} \Delta_{jk}}$$

which leads to the claim that $\mathbf{J}_e^{\text{II}}(\mathbf{p}_k) \preceq \mathbf{J}_e^{\text{I}}(\mathbf{p}_k)$.

APPENDIX D PROOF OF PROPOSITION 6

Consider the following problem

$$\begin{aligned} & \tilde{\mathcal{P}}_{\text{aux},1}^{(k)} : \min_{\mathbf{M} \in \mathbb{R}^{2 \times 2}, \{x_{jk}, y_j\}_{j \in \mathcal{N}_a \setminus \{k\}}} \text{tr}\{\mathbf{M}\} \\ & \text{s.t. } y_j = \frac{x_{jk} \xi_{jk}}{1 + x_{jk} \xi_{jk} \Delta_{jk}^R}, \\ & \quad j \in \mathcal{N}_a \setminus \{k\} \quad (27) \end{aligned}$$

(4), (5) and (17).

Analogously to Proposition 5, one can show that $\tilde{\mathcal{P}}_{\text{aux},1}^{(k)}$ is equivalent to $\mathcal{P}_{\text{agt},1}^{(k)}$ and they have the same minimum objective value. Hence, we only need to prove that $\tilde{\mathcal{P}}_{\text{aux},1}^{(k)}$ and $\mathcal{P}_{\text{aux},1}^{(k)}$ have the same minimum objective value and that the optimal solution of $\tilde{\mathcal{P}}_{\text{aux},1}^{(k)}$ can be obtained from that of $\mathcal{P}_{\text{aux},1}^{(k)}$.

On the one hand, since (18) is a relaxed constraint of (27), the minimum objective value of $\mathcal{P}_{\text{aux},1}^{(k)}$ is no greater than that of $\tilde{\mathcal{P}}_{\text{aux},1}^{(k)}$. On the other hand, for an optimal solution $\{\mathbf{M}^*, \{x_{jk}^*, y_j^*\}_{j \in \mathcal{N}_a \setminus \{k\}}\}$ of $\mathcal{P}_{\text{aux},1}^{(k)}$, there exists $\{\tilde{x}_{jk}^*\}_{j \in \mathcal{N}_a \setminus \{k\}}$ such that $\tilde{x}_{jk}^* \leq x_{jk}^*$ and

$$y_j^* = \frac{\tilde{x}_{jk}^* \xi_{jk}}{1 + \tilde{x}_{jk}^* \xi_{jk} \Delta_{jk}^R} \quad (28)$$

due to that $x \xi_{jk} / (1 + x \xi_{jk} \Delta_{jk}^R)$ is an increasing function of x . Hence, $\{\mathbf{M}^*, \{\tilde{x}_{jk}^*, y_j^*\}_{j \in \mathcal{N}_a \setminus \{k\}}\}$ is also an optimal solution of $\tilde{\mathcal{P}}_{\text{aux},1}^{(k)}$. In the meantime, (28) implies that $\{\mathbf{M}^*, \{\tilde{x}_{jk}^*, y_j^*\}_{j \in \mathcal{N}_a \setminus \{k\}}\}$ is a feasible solution of $\tilde{\mathcal{P}}_{\text{aux},1}^{(k)}$ and hence the minimum objective value of $\tilde{\mathcal{P}}_{\text{aux},1}^{(k)}$ is no greater than $\text{tr}\{\mathbf{M}^*\}$, which is the minimum objective value of $\mathcal{P}_{\text{aux},1}^{(k)}$.

Therefore, $\mathcal{P}_{\text{aux},1}^{(k)}$ and $\tilde{\mathcal{P}}_{\text{aux},1}^{(k)}$ have the same minimum objective value and the $\{\mathbf{M}^*, \{\tilde{x}_{jk}^*, y_j^*\}_{j \in \mathcal{N}_a \setminus \{k\}}\}$ is the optimal solution of $\tilde{\mathcal{P}}_{\text{aux},1}^{(k)}$, obtained from that of $\mathcal{P}_{\text{aux},1}^{(k)}$. This concludes the proof of Proposition 6.

$$\mathbf{J}_e^L(\mathbf{p}) = \begin{bmatrix} \mathbf{J}_e^A(\mathbf{p}_1) + \sum_{j \in \mathcal{N}_a \setminus \{1\}} \mathbf{C}_{1,j} & -\mathbf{C}_{1,2} & \cdots & -\mathbf{C}_{1,N_a} \\ -\mathbf{C}_{2,1} & \mathbf{J}_e^A(\mathbf{p}_2) + \mathbf{C}_{2,1} & & \mathbf{0} \\ \vdots & & \ddots & \\ -\mathbf{C}_{N_a,1} & \mathbf{0} & & \mathbf{J}_e^A(\mathbf{p}_{N_a}) + \mathbf{C}_{N_a,1} \end{bmatrix} \quad (23)$$

APPENDIX E
PROOF OF PROPOSITION 7

Let \mathbf{y}_k^* denote an optimal APAV for $\mathcal{P}_{\text{anc}}^{(k)}$ with the minimum number of positive elements and let $m = \|\mathbf{y}_k^*\|_0$. If there are multiple such vectors, any can be chosen. Without loss of generality, consider that the first m elements of \mathbf{y}_k^* are positive, i.e.,

$$\mathbf{y}_k^* = [(\mathbf{y}^*)^T \quad \mathbf{0}_{N_b-m}^T]^T \quad (29)$$

where \mathbf{y}^* denotes the vector consisting of the m positive elements of \mathbf{y}_k^* . Let $\mathbf{R} = \text{diag}\{\xi_{k(N_a+1)}, \xi_{k(N_a+2)} \cdots, \xi_{k(N_a+m)}\}$ and Λ be the first principle $m \times m$ matrix of Λ_k , i.e.,

$$\Lambda = \mathbf{1}\mathbf{1}^T - \mathbf{c}\mathbf{c}^T - \mathbf{s}\mathbf{s}^T$$

with

$$\begin{aligned} \mathbf{c} &= [\cos \phi_{k(N_a+1)} \quad \cos \phi_{k(N_a+2)} \quad \cdots \quad \cos \phi_{k(N_a+m)}]^T \\ \mathbf{s} &= [\sin \phi_{k(N_a+1)} \quad \sin \phi_{k(N_a+2)} \quad \cdots \quad \sin \phi_{k(N_a+m)}]^T. \end{aligned}$$

If $m \leq \text{rank}\{\Lambda_k\}$, the proof is complete; otherwise, it will lead to a contradiction shown as follows.

If $m > \text{rank}\{\Lambda_k\}$, then $m > \text{rank}\{\Lambda\}$ since $\text{rank}\{\Lambda_k\} \geq \text{rank}\{\Lambda\}$. This gives $\mathbf{I} - \Lambda^+ \Lambda \neq \mathbf{0}$, which is equivalent to $\mathbf{I} - \mathbf{R}^{-1} \Lambda^+ \Lambda \mathbf{R} \neq \mathbf{0}$. Suppose the l th column of $(\mathbf{I} - \mathbf{R}^{-1} \Lambda^+ \Lambda \mathbf{R})$ is not $\mathbf{0}$. Consider the following mapping

$$\mathbf{g}(t) = \mathbf{y}^* + t \cdot (\mathbf{I} - \mathbf{R}^{-1} \Lambda^+ \Lambda \mathbf{R}) \mathbf{e}_l$$

where $\mathbf{e}_l \in \mathbb{R}^m$. By Lemma 1 (shown in Appendix F), there exists \tilde{t} such that $\mathbf{g}(\tilde{t}) \geq \mathbf{0}$ and $\|\mathbf{g}(\tilde{t})\|_0 < m$. Then consider the APAV $\tilde{\mathbf{y}}_k = [\mathbf{g}(\tilde{t})^T \quad \mathbf{0}^T]^T$. By Lemma 2 (shown in Appendix G), $\tilde{\mathbf{y}}_k$ is an optimal APAV for $\mathcal{P}_{\text{anc}}^{(k)}$. However, $\|\tilde{\mathbf{y}}_k\|_0 < m$, which contradicts that \mathbf{y}_k^* is the optimal APAV with the minimum number of positive elements.

APPENDIX F

Lemma 1: Given $n \in \mathbb{N}$ and $\mathbf{w}, \mathbf{z} \in \mathbb{R}^n$, if $\mathbf{w} \succ \mathbf{0}$ and $\mathbf{z} \neq \mathbf{0}$, there exists $\tilde{t} \in \mathbb{R}$ such that $\mathbf{w} + \tilde{t}\mathbf{z} \geq \mathbf{0}$ and $\|\mathbf{w} + \tilde{t}\mathbf{z}\|_0 < n$.

Proof: This lemma can be proved by considering a mapping $f: \mathbb{R} \rightarrow \mathbb{R}^n$

$$f(t) = \mathbf{w} + t\mathbf{z}.$$

Note that (i) $f(0) = \mathbf{w}$ is a vector with all positive elements; (ii) either $f(t)$ or $f(-t)$ has at least one negative element for sufficiently large t ; (iii) $f(\cdot)$ is continuous on t . Thus, there exists $\tilde{t} \in \mathbb{R}$ such that $f(\tilde{t}) \geq \mathbf{0}$ with $f(\tilde{t})$ containing at least one zero element, i.e., $\|f(\tilde{t})\|_0 < n$. \square

APPENDIX G

Lemma 2: If $\mathbf{y} = \mathbf{y}^* + (\mathbf{I} - \mathbf{R}^{-1} \Lambda^+ \Lambda \mathbf{R})\mathbf{w}$, where \mathbf{y}^* is given in (29), and $\mathbf{w} \in \mathbb{R}^m$ is an arbitrary real vector satisfying $\mathbf{y} \geq \mathbf{0}$, then $\mathbf{y}_k = [\mathbf{y}^T \quad \mathbf{0}_{N_b-m}^T]^T$ is an optimal APAV for $\mathcal{P}_{\text{anc}}^{(k)}$.

Proof: To prove \mathbf{y}_k is an optimal APAV for $\mathcal{P}_{\text{anc}}^{(k)}$, it suffices to prove that \mathbf{y}_k achieves the same SPEB as \mathbf{y}_k^* in (29) and that \mathbf{y}_k satisfies the total power constraint.

One can verify that $\mathbf{1} \in \text{span}\{\text{columns of } \Lambda\}$ and hence $\mathbf{1}^T (\mathbf{I} - \Lambda^+ \Lambda) = \mathbf{0}^T$. Consequently,

$$\mathbf{1}^T \mathbf{R} (\mathbf{I} - \mathbf{R}^{-1} \Lambda^+ \Lambda \mathbf{R}) = \mathbf{0}^T. \quad (30)$$

Note that

$$\mathbf{1}_{N_b}^T \mathbf{R}_k \mathbf{y}_k \stackrel{(a)}{=} \mathbf{1}_m^T \mathbf{R} \mathbf{y} \stackrel{(b)}{=} \mathbf{1}_m^T \mathbf{R} \mathbf{y}^* \stackrel{(c)}{=} \mathbf{1}_{N_b}^T \mathbf{R}_k \mathbf{y}_k^* \quad (31)$$

where (a) is due to the relationship between \mathbf{y}_k and \mathbf{y} , (b) is due to (30), and (c) is due to (29). By the definition of the pseudo-inverse matrix, $\Lambda(\mathbf{I} - \Lambda^+ \Lambda) = \mathbf{0}$. Consequently,

$$\mathbf{R} \Lambda \mathbf{R} (\mathbf{I} - \mathbf{R}^{-1} \Lambda^+ \Lambda \mathbf{R}) = \mathbf{0}. \quad (32)$$

Note that

$$\begin{aligned} (\mathbf{y}_k)^T \mathbf{R}_k \Lambda_k \mathbf{R}_k \mathbf{y}_k &\stackrel{(d)}{=} (\mathbf{y})^T \mathbf{R} \Lambda \mathbf{R} \mathbf{y} \\ &\stackrel{(e)}{=} (\mathbf{y}^*)^T \mathbf{R} \Lambda \mathbf{R} \mathbf{y}^* \\ &\stackrel{(f)}{=} (\mathbf{y}_k^*)^T \mathbf{R}_k \Lambda_k \mathbf{R}_k \mathbf{y}_k^* \end{aligned} \quad (33)$$

where (d) is due to the relationship between \mathbf{y}_k and \mathbf{y} , (e) is due to (32), and (f) is due to (29). Recalling the SPEB expression in (19), equations (31) and (33) imply that \mathbf{y}_k and \mathbf{y}_k^* achieve the same SPEB, i.e., $\mathcal{P}^A(\mathbf{p}_k; \mathbf{y}_k) = \mathcal{P}^A(\mathbf{p}_k; \mathbf{y}_k^*)$.

If $\mathbf{1}^T (\mathbf{I} - \mathbf{R}^{-1} \Lambda^+ \Lambda \mathbf{R}) = \mathbf{0}^T$, then $\mathbf{1}^T \mathbf{y}_k = \mathbf{1}^T \mathbf{y}_k^*$, indicating that \mathbf{y}_k satisfies the power constraint (4) and hence the proof is complete; otherwise, it will lead to a contradiction shown as follows.

If $\mathbf{1}^T (\mathbf{I} - \mathbf{R}^{-1} \Lambda^+ \Lambda \mathbf{R}) \neq \mathbf{0}^T$, then there exists $\mathbf{w}_s \neq \mathbf{0}$ such that $\mathbf{1}^T (\mathbf{I} - \mathbf{R}^{-1} \Lambda^+ \Lambda \mathbf{R}) \mathbf{w}_s < 0$. Moreover, there exists a sufficiently small $\beta > 0$ such that $\mathbf{y}^* + (\mathbf{I} - \mathbf{R}^{-1} \Lambda^+ \Lambda \mathbf{R}) \beta \mathbf{w}_s \geq \mathbf{0}$ since $\mathbf{y}^* \succ \mathbf{0}$. Let $\mathbf{w} = \beta \mathbf{w}_s$ and then the corresponding \mathbf{y} and \mathbf{y}_k satisfy that

$$\mathbf{1}_{N_b}^T \mathbf{y}_k = \mathbf{1}_m^T \mathbf{y} < \mathbf{1}_m^T \mathbf{y}^* = \mathbf{1}_{N_b}^T \mathbf{y}_k^*.$$

Consider a scaled APAV $\tilde{\mathbf{y}}_k = \mathbf{y}_k / \gamma$ where

$$\gamma = (\mathbf{1}^T \mathbf{y}_k) / (\mathbf{1}^T \mathbf{y}_k^*).$$

One can verify that

$$\begin{aligned} \mathcal{P}^A(\mathbf{p}_k; \tilde{\mathbf{y}}_k) &= \mathcal{P}^A(\mathbf{p}_k; \mathbf{y}_k / \gamma) \\ &= \gamma \mathcal{P}^A(\mathbf{p}_k; \mathbf{y}_k) \stackrel{(g)}{<} \mathcal{P}^A(\mathbf{p}_k; \mathbf{y}_k) \\ &= \mathcal{P}^A(\mathbf{p}_k; \mathbf{y}_k^*) \end{aligned} \quad (34)$$

where (g) is true since $\gamma < 1$. Equation (34) implies $\tilde{\mathbf{y}}_k$ outperforms \mathbf{y}_k^* , which contradicts the fact that \mathbf{y}_k^* is an optimal APAV. \square

ACKNOWLEDGMENTS

The authors would like to thank A. Conti and R. Cohen for their valuable suggestions and careful reading of the manuscript.

REFERENCES

- [1] M. Z. Win, A. Conti, S. Mazuelas, Y. Shen, W. M. Gifford, D. Dardari, and M. Chiani, "Network localization and navigation via cooperation," *IEEE Commun. Mag.*, vol. 49, no. 5, pp. 56–62, May 2011.
- [2] Y. Shen, S. Mazuelas, and M. Z. Win, "Network navigation: Theory and interpretation," *IEEE J. Sel. Areas Commun.*, vol. 30, no. 9, pp. 1823–1834, Oct. 2012.
- [3] A. H. Sayed, A. Tarighat, and N. Khajehnouri, "Network-based wireless location: Challenges faced in developing techniques for accurate wireless location information," *IEEE Signal Process. Mag.*, vol. 22, no. 4, pp. 24–40, Jul. 2005.
- [4] K. Pahlavan, X. Li, and J.-P. Mäkelä, "Indoor geolocation science and technology," *IEEE Commun. Mag.*, vol. 40, no. 2, pp. 112–118, Feb. 2002.
- [5] N. Patwari, J. N. Ash, S. Kyperountas, A. O. Hero, R. L. Moses, and N. S. Correal, "Locating the nodes: Cooperative localization in wireless sensor networks," *IEEE Signal Process. Mag.*, vol. 22, no. 4, pp. 54–69, Jul. 2005.
- [6] S. Gezici, Z. Tian, G. B. Giannakis, H. Kobayashi, A. F. Molisch, H. V. Poor, and Z. Sahinoglu, "Localization via ultra-wideband radios: A look at positioning aspects for future sensor networks," *IEEE Signal Process. Mag.*, vol. 22, no. 4, pp. 70–84, Jul. 2005.
- [7] J. J. Caffery and G. L. Stüber, "Overview of radiolocation in CDMA cellular systems," *IEEE Commun. Mag.*, vol. 36, no. 4, pp. 38–45, Apr. 1998.
- [8] Y. Shen and M. Z. Win, "Fundamental limits of wideband localization – Part I: A general framework," *IEEE Trans. Inf. Theory*, vol. 56, no. 10, pp. 4956–4980, Oct. 2010.
- [9] D. Dardari, A. Conti, C. Buratti, and R. Verdone, "Mathematical evaluation of environmental monitoring estimation error through energy-efficient wireless sensor networks," *IEEE Trans. Mobile Comput.*, vol. 6, no. 7, pp. 790–802, Jul. 2007.
- [10] J. J. Spilker, Jr., "GPS signal structure and performance characteristics," *Journal of the Institute of Navigation*, vol. 25, no. 2, pp. 121–146, Summer 1978.
- [11] S. Mazuelas, Y. Shen, and M. Z. Win, "Belief condensation filtering," *IEEE Trans. Signal Process.*, vol. 61, no. 18, pp. 4403–4415, Sep. 2013.
- [12] K. Plarre and P. R. Kumar, "Tracking objects with networked scattered directional sensors," *EURASIP J. Adv. in Signal Process.*, vol. 2008, no. 74, pp. 1–10, Jan. 2008.
- [13] R. Verdone, D. Dardari, G. Mazzini, and A. Conti, *Wireless Sensor and Actuator Networks: Technologies, Analysis and Design*. Amsterdam, The Netherlands: Elsevier, 2008.
- [14] A. Rabbachin, I. Oppermann, and B. Denis, "GML ToA estimation based on low complexity UWB energy detection," in *Proc. IEEE Int. Symp. on Personal, Indoor and Mobile Radio Commun.*, Helsinki, Finland, Sep. 2006, pp. 1–5.
- [15] D. B. Jourdan, D. Dardari, and M. Z. Win, "Position error bound for UWB localization in dense cluttered environments," *IEEE Trans. Aerosp. Electron. Syst.*, vol. 44, no. 2, pp. 613–628, Apr. 2008.
- [16] J. Xu, X. Shen, J. W. Mark, and J. Cai, "Mobile location estimation in CDMA cellular networks by using fuzzy logic," *Wireless Communications and Mobile Computing*, vol. 7, no. 3, pp. 285–298, Mar. 2007.
- [17] J. Luo and Q. Zhang, "Relative distance based localization for mobile sensor networks," in *Proc. IEEE Global Telecomm. Conf.*, Washington, DC, Nov. 2007, pp. 1076–1080.
- [18] A. Conti, M. Guerra, D. Dardari, N. Decarli, and M. Z. Win, "Network experimentation for cooperative localization," *IEEE J. Sel. Areas Commun.*, vol. 30, no. 2, pp. 467–475, Feb. 2012.
- [19] B. Alavi and K. Pahlavan, "Modeling of the TOA-based distance measurement error using UWB indoor radio measurements," *IEEE Commun. Lett.*, vol. 10, no. 4, pp. 275–277, Apr. 2006.
- [20] A. Conti, D. Dardari, M. Guerra, L. Mucchi, and M. Z. Win, "Experimental characterization of diversity navigation," *IEEE Syst. J.*, vol. 8, no. 1, pp. 115–124, Mar. 2014.
- [21] L. Mailaender, "On the geolocation bounds for round-trip time-of-arrival and all non-line-of-sight channels," *EURASIP J. Adv. in Signal Process.*, vol. 2008, pp. 1–10, 2008.
- [22] D. Dardari, A. Conti, U. J. Ferner, A. Giorgetti, and M. Z. Win, "Ranging with ultrawide bandwidth signals in multipath environments," *Proc. IEEE*, vol. 97, no. 2, pp. 404–426, Feb. 2009.
- [23] S. Mazuelas, R. M. Lorenzo, A. Bahillo, P. Fernandez, J. Prieto, and E. J. Abril, "Topology assessment provided by weighted barycentric parameters in harsh environment wireless location systems," *IEEE Trans. Signal Process.*, vol. 58, no. 7, pp. 3842–3857, Jul. 2010.
- [24] P. Tichavský, C. H. Muravchik, and A. Nehorai, "Posterior Cramér-Rao bounds for discrete-time nonlinear filtering," *IEEE Trans. Signal Process.*, vol. 46, no. 5, pp. 1386–1396, May 1998.
- [25] Y. Shen, H. Wymeersch, and M. Z. Win, "Fundamental limits of wideband localization – Part II: Cooperative networks," *IEEE Trans. Inf. Theory*, vol. 56, no. 10, pp. 4981–5000, Oct. 2010.
- [26] X. Tan and J. Li, "Cooperative positioning in underwater sensor networks," *IEEE Trans. Signal Process.*, vol. 58, no. 11, pp. 5860–5871, Nov. 2010.
- [27] H. Wymeersch, J. Lien, and M. Z. Win, "Cooperative localization in wireless networks," *Proc. IEEE*, vol. 97, no. 2, pp. 427–450, Feb. 2009.
- [28] C. Chang and A. Sahai, "Cramér-Rao-type bounds for localization," *EURASIP J. Appl. Signal Process.*, vol. 2006, pp. Article ID 94 287, 13 pages, 2006.
- [29] Y. Shen and M. Z. Win, "Energy efficient location-aware networks," in *Proc. IEEE Int. Conf. Commun.*, Beijing, China, May 2008, pp. 2995–3001.
- [30] S. Jeong, O. Simeone, A. M. Haimovich, and J. Kang, "Beamforming design for joint localization and data transmission in distributed antenna system," *IEEE Trans. Veh. Technol.*, vol. pp, no. 99, pp. 1–15, Apr. 2014.
- [31] G. Alirezaei, M. Reyer, and R. Mathar, "Optimum power allocation in sensor networks for passive radar applications," *IEEE Trans. Wireless Commun.*, vol. 13, no. 6, pp. 3222–3231, Jun. 2014.
- [32] T. Wang, G. Leus, and L. Huang, "Ranging energy optimization for robust sensor positioning based on semidefinite programming," *IEEE Trans. Signal Process.*, vol. 57, no. 12, pp. 4777–4787, Dec. 2009.
- [33] H. Godrich, A. P. Petropulu, and H. V. Poor, "Power allocation strategies for target localization in distributed multiple-radar architectures," *IEEE Trans. Signal Process.*, vol. 59, no. 7, pp. 3226–3240, Jul. 2011.
- [34] W. W.-L. Li, Y. Shen, Y. J. Zhang, and M. Z. Win, "Robust power allocation for energy-efficient location-aware networks," *IEEE/ACM Trans. Netw.*, vol. 21, no. 6, pp. 1918–1930, Dec. 2013.
- [35] Y. Shen, W. Dai, and M. Z. Win, "Power optimization for network localization," *IEEE/ACM Trans. Netw.*, vol. 22, no. 4, pp. 1337–1350, Aug. 2014.
- [36] U. A. Khan and J. M. F. Moura, "Distributing the Kalman filter for large-scale systems," *IEEE Trans. Signal Process.*, vol. 56, no. 10, pp. 4919–4935, Oct. 2008.
- [37] U. A. Khan, S. Kar, and J. M. F. Moura, "Distributed sensor localization in random environments using minimal number of anchor nodes," *IEEE Trans. Signal Process.*, vol. 57, no. 5, pp. 2000–2016, May 2009.
- [38] —, "DILAND: An algorithm for distributed sensor localization with noisy distance measurements," *IEEE Trans. Signal Process.*, vol. 58, no. 3, pp. 1940–1947, Mar. 2010.
- [39] S. Mazuelas, Y. Shen, and M. Z. Win, "Information coupling in cooperative localization," *IEEE Commun. Lett.*, vol. 15, no. 7, pp. 737–739, Jul. 2011.
- [40] P. J. Bickel and K. Doksum, *Mathematical Statistics: Basic Ideas and Selected Topics*, 2nd ed. Upper Saddle River, NJ: Prentice Hall, 2001, vol. 1.
- [41] H. L. Van Trees, *Detection, Estimation and Modulation Theory, Part I*. New York, NY: Wiley, 1968.
- [42] H. V. Poor, *An Introduction to Signal Detection and Estimation*, 2nd ed. New York: Springer-Verlag, 1994.
- [43] W. Dai, "Geometric Methods for Optimal Resource Allocation in Wireless Network Localization," Master's thesis, Department of Aeronautics and Astronautics, Massachusetts Institute of Technology, Cambridge, MA, Jun. 2014.
- [44] M. Grant and S. Boyd, "CVX: Matlab software for disciplined convex programming, version 1.21," <http://cvxr.com/cvx>, Aug. 2010.
- [45] "Winner II interim channel models," *IST-4-027756 WINNER II D1.1.2 v1.2*, Sep. 2007.
- [46] *Technical Specification LTE; Evolved Universal Terrestrial Radio Access (E-UTRA); User Equipment (UE) radio transmission and reception*, 3rd Generation Partnership Project 3GPP™ TS 136.101 V11.2.0 (2012-11), Nov. 2012, release 11.
- [47] W. Dai, Y. Shen, and M. Z. Win, "Energy efficient cooperative network localization," in *Proc. IEEE Int. Conf. Commun.*, Sydney, Australia, Jun. 2014.
- [48] S. Boyd and L. Vandenberghe, *Convex Optimization*. Cambridge, UK: Cambridge University Press, 2004.



Wenhan Dai (S'12) received the B.S. degrees in electronic engineering and in mathematics from Tsinghua University, Beijing, China, in 2011, and received the S.M. degree in aeronautics and astronautics at the Massachusetts Institute of Technology (MIT), Cambridge, MA, USA, in 2014.

Since 2011, he has been a research assistant with Wireless Communications and Network Science Laboratory, MIT, where he is currently pursuing the Ph.D. degree. His research interests include communication theory, stochastic optimization, and their application to wireless communication and network localization. His current research focuses on resource allocation for network localization, cooperative network operation, and ultra-wide bandwidth communications.

He served as a reviewer for IEEE TRANSACTIONS ON WIRELESS COMMUNICATIONS and IEEE JOURNAL ON SELECTED AREAS IN COMMUNICATIONS. He received the academic excellence scholarships from 2008 to 2010 and the Outstanding Thesis Award in 2011 from Tsinghua University.



Yuan Shen (S'05-M'14) received the B.E. degree (*with highest honor*) in electronic engineering from Tsinghua University, China, in 2005, and the S.M. degree and the Ph.D. degree in electrical engineering and computer science from the Massachusetts Institute of Technology (MIT), Cambridge, in 2008 and 2014, respectively.

Since 2014, he is a postdoctoral associate with the Laboratory for Information and Decision Systems (LIDS) at MIT, Cambridge, MA. He joined the Department of Electronic Engineering at Tsinghua University, Beijing as an Associate Professor in June 2014. He was with the Wireless Communication and Network Sciences Laboratory at MIT in 2005–2014, the Wireless Communications Laboratory at The Chinese University of Hong Kong in summer 2010, the Hewlett-Packard Labs in winter 2009, the Corporate R&D at Qualcomm Inc. in summer 2008, and the A&D Center at Texas Instrument in summer 2004. His research interests include statistical inference, network science, communication theory, and information theory. His current research focuses on network localization and navigation, generalized filtering techniques, resource allocation, intrinsic wireless secrecy, and cooperative networks.

Dr. Shen served as a member of the Technical Program Committee (TPC) for the IEEE Globecom in (2010–2014), the IEEE ICC in (2010–2015), the IEEE WCNC in (2009–2015), the IEEE ICUWB in (2011–2014), the IEEE ICC in 2012 and 2014, and CHINACOM in 2014. He was a recipient of the China's Youth 1000-Talent Program (2014), the Marconi Society Paul Baran Young Scholar Award (2010), the MIT EECS Ernst A. Guillemin Best S.M. Thesis Award (2008), the Qualcomm Roberto Padovani Scholarship (2008), and the MIT Walter A. Rosenblith Presidential Fellowship (2005). His papers received the IEEE Communications Society Fred W. Ellersick Prize (2012) and three Best Paper Awards from the IEEE Globecom (2011), the IEEE ICUWB (2011), and the IEEE WCNC (2007).



Moe Z. Win (S'85-M'87-SM'97-F'04) received both the Ph.D. in Electrical Engineering and the M.S. in Applied Mathematics as a Presidential Fellow at the University of Southern California (USC) in 1998. He received the M.S. in Electrical Engineering from USC in 1989 and the B.S. (*magna cum laude*) in Electrical Engineering from Texas A&M University in 1987.

He is a Professor at the Massachusetts Institute of Technology (MIT) and the founding director of the Wireless Communication and Network Sciences Laboratory. Prior to joining MIT, he was with AT&T Research Laboratories for five years and with the Jet Propulsion Laboratory for seven years. His research encompasses fundamental theories, algorithm design, and experimentation for a broad range of real-world problems. His current research topics include network localization and navigation, network interference exploitation, intrinsic wireless secrecy, adaptive diversity techniques, and ultra-wide bandwidth systems.

Professor Win is an elected Fellow of the AAAS, the IEEE, and the IET, and was an IEEE Distinguished Lecturer. He was honored with two IEEE Technical Field Awards: the IEEE Kiyo Tomiyasu Award (2011) and the IEEE Eric E. Sumner Award (2006, jointly with R. A. Scholtz). Together with students and colleagues, his papers have received numerous awards, including the IEEE Communications Society's Stephen O. Rice Prize (2012), the IEEE Aerospace and Electronic Systems Society's M. Barry Carlton Award (2011), the IEEE Communications Society's Guglielmo Marconi Prize Paper Award (2008), and the IEEE Antennas and Propagation Society's Sergei A. Schelkunoff Transactions Prize Paper Award (2003). Highlights of his international scholarly initiatives are the Copernicus Fellowship (2011), the Royal Academy of Engineering Distinguished Visiting Fellowship (2009), and the Fulbright Fellowship (2004). Other recognitions include the International Prize for Communications Cristoforo Colombo (2013), the *Laurea Honoris Causa* from the University of Ferrara (2008), the Technical Recognition Award of the IEEE ComSoc Radio Communications Committee (2008), and the U.S. Presidential Early Career Award for Scientists and Engineers (2004).

Dr. Win was an elected Member-at-Large on the IEEE Communications Society Board of Governors (2011–2013). He was the Chair (2004–2006) and Secretary (2002–2004) for the Radio Communications Committee of the IEEE Communications Society. Over the last decade, he has organized and chaired numerous international conferences. He is currently an Editor-at-Large for the IEEE WIRELESS COMMUNICATIONS LETTERS and is serving on the Editorial Advisory Board for the IEEE TRANSACTIONS ON WIRELESS COMMUNICATIONS. He served as Editor (2006–2012) for the IEEE TRANSACTIONS ON WIRELESS COMMUNICATIONS, and as Area Editor (2003–2006) and Editor (1998–2006) for the IEEE TRANSACTIONS ON COMMUNICATIONS. He was Guest-Editor for the PROCEEDINGS OF THE IEEE (2009) and for the IEEE JOURNAL ON SELECTED AREAS IN COMMUNICATIONS (2002).